

Stoichiometric Self-Assembly of Shape-Persistent 2D Complexes: A Facile Route to a Symmetric Supramacromolecular Spoked Wheel

Jin-Liang Wang,^{†,§} Xiaopeng Li,^{‡,§} Xiaocun Lu,[†] I-Fan Hsieh,[†] Yan Cao,[†] Charles N. Moorefield,[†] Chrys Wesdemiotis,^{*,†,‡} Stephen Z. D. Cheng,[†] and George R. Newkome^{*,†,‡}

[†]Department of Polymer Science and [‡]Department of Chemistry, The University of Akron, Akron, Ohio 44325, United States

 Supporting Information

ABSTRACT: An approach to multicomponent coordination-driven self-assembly of the first terpyridine-based, shape-persistent, giant two-dimensional D_{6h} supramacromolecular spoked wheel is reported. Mixing core **T6**, rim **T3**, and Zn^{II} or Cd^{II} ions in a stoichiometric ratio (1:6:12) permitted the selective generation of a highly symmetric spoked wheel in 94% isolated yield via geometric and thermodynamic control. The products were characterized by a combination of traveling-wave ion mobility mass spectrometry and NMR techniques together with TEM imaging, which agreed with computational simulations.

The spontaneous and precise self-assembly of multiple distinct subunits is used in Nature to create many functional biological systems with well-defined geometries.¹ To simulate and simplify Nature's complexity, coordination-driven self-assembly has been developed as a strategy for constructing abiological supramolecular two-dimensional (2D)² and three-dimensional (3D)³ architectures with precise shapes and sizes. However, use of multicomponent systems possesses the inherent weakness that multiple equilibria can generate multiple similar structures.⁴ These assemblies mainly rely on specific stoichiometry, the shape information instilled in the components, and the reaction conditions.⁵ Although such structures are easily designed, construction of a single discrete structure within a mixture by multicomponent self-assembly is still a synthetic challenge.⁶

In the coordination-driven approach to supramolecular chemistry, 2,2':6',2''-terpyridine (tpy)-based building blocks have attracted considerable interest because of their inherent ability to bind transition-metal ions strongly and the relative ease of functionalizing connectors for multinuclear assemblies.⁷ Hexameric ring-shaped structures are found in many functional biological systems, such as the family of ATPases, DNA hexameric helicases, and HIV capsid.⁸ These biological superstructures have inspired the use of 3,5-bis(terpyridine)benzene ligands possessing a 120° angle to construct a family of utilitarian metallomacrocycles based on <tpy–M^{II}–tpy> connectivity.⁹ In addition to the dominant hexagonal shape, other macromolecular family members (squares to cyclododecamers) have also recently been generated using this simple one-step strategy.¹⁰ Thus, the concept of a molecular wheel consisting of a hub unit, stable directed spokes, and a circular rim has been used for the synthesis of large, monodisperse covalent macrocycles, as this can simplify the

synthetic route and increase the yield.¹¹ Nevertheless, a supramolecular spoked wheel with a continuous outer wheel rim based solely on noncovalent interactions has not been reported to date because of a dearth of appropriate supporting spoke and rim elements for preorganization.¹² To address this problem, we herein describe a stoichiometric self-assembly algorithm for the construction of a shape-persistent 2D supramacromolecular spoked wheel possessing D_{6h} symmetry in nearly quantitative yield in a one-pot reaction.

The design rationale for multicomponent coordination-driven self-assembly of the molecular spoked wheel [**T6**₁–**Cd**₁₂–**T3**₆] (Figure 1) is outlined in Scheme 1. Formation of this giant wheel possessing sixfold symmetry required only Cd^{II} ions and two different building blocks. The three-armed outer ligand **T3** was designed to incorporate (1) three tpy groups that simultaneously generate half of one spoke and one-sixth of the outer wheel and (2) three methoxy moieties (2:1 ratio) to enhance the solubility and serve as markers to permit easy analysis of the inherent D_{6h} symmetry. The hub **T6** instills D_{6h} symmetry as well as the other half of each directed molecular spoke upon formation of the <tpy– Cd^{II} –tpy> linkages. In view of the high stability of highly symmetric structures having multiple (>2) interlocking connections within each ligand,^{3c} we hypothesized that the stability of this symmetric wheel would be enhanced oversimpler byproducts on the basis of the three or six noncovalent interactions within each ligand. Additionally, we assumed these multiple interactions within the designed geometry would facilitate the formation of a single, discrete architecture.

Boronic acid **2** (Scheme 1) was synthesized (64%) from unprotected 4-formylphenylboronic acid by a known procedure.¹³ Ligand **T3** was prepared (61%) from **2** and **1** by a threefold Suzuki coupling reaction using $Pd(PPh_3)_4$ as the catalyst. Interestingly, the 1:2 ratio of singlets (4.14 and 3.73 ppm; $\Delta\delta = 0.41$ ppm) for the methoxy groups in **T3** were easily discernible from those of **1** (3.94 and 3.90 ppm; $\Delta\delta = 0.04$ ppm) because of the upfield shift caused by the adjacent phenyl rings together with steric congestion. Moreover, the aromatic region of **T3** showed two sets of protons in a 2:1 ratio belonging to the tpy branches and the phenyl groups (Figure 2). The core **T6**¹⁴ was synthesized (41% isolated yield) by a sixfold reaction utilizing Suzuki coupling of hexabromobenzene and **2** catalyzed by $Pd(PPh_3)_4$.

Since compositional reversibility and the strength of the <tpy–M^{II}–tpy> linkages is important for kinetically controlled generation of heteroleptic complexes, either Zn^{II} or Cd^{II} is the

Received: May 2, 2011

Published: June 09, 2011

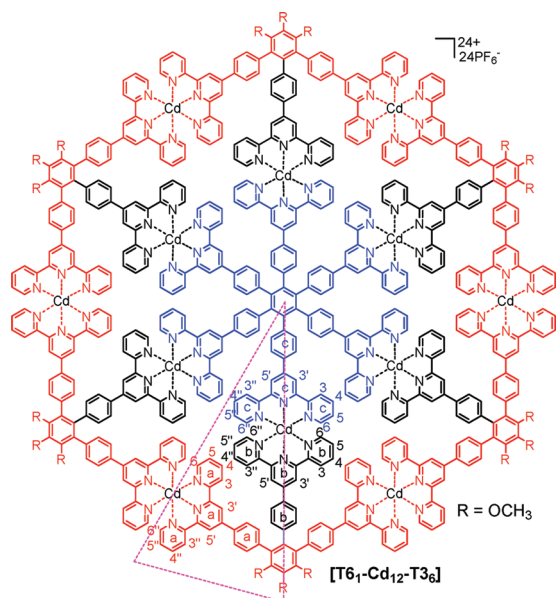
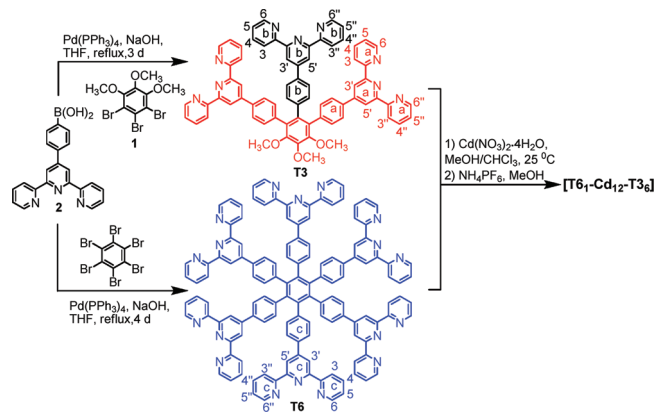


Figure 1. Structure of the supramacromolecular spoked wheel $[\text{T6}_1-\text{Cd}_{12}-\text{T3}_6]$; the triangle denotes the smallest subunit.

Scheme 1. Synthetic Route to the Ligands and $[\text{T6}_1-\text{Cd}_{12}-\text{T3}_6]$.



most appropriate metal choice.^{7,9,15} The initial efforts utilized core **T6**, rim **T3**, and $\text{Zn}(\text{NO}_3)_2 \cdot 6\text{H}_2\text{O}$ in a precise stoichiometric ratio of 1:6:12 to form the desired molecular wheel $[\text{T6}_1-\text{Zn}_{12}-\text{T3}_6]$; although it did form, some homo-oligomeric byproducts were evident by NMR and electrospray ionization mass spectrometry (ESI-MS) analysis [see Figures S1–S4 (SI)]. Therefore, Cd^{II} reagents were used to see whether the weaker bonds would favor the formation of the desired wheel in higher purity. The reaction of core **T6**, rim **T3**, and $\text{Cd}(\text{NO}_3)_2 \cdot 4\text{H}_2\text{O}$ (1:6:12) in $\text{CHCl}_3/\text{MeOH}$ solution at 25 °C for 30 min followed by the addition of excess NH_4PF_6 generated the anticipated wheel $[\text{T6}_1-\text{Cd}_{12}-\text{T3}_6]$ in 94% isolated yield. This assembled product showed excellent solubility in MeCN, acetone, and *N,N*-dimethylformamide and was stable at ambient temperatures.

The ^1H NMR spectrum of $[\text{T6}_1-\text{Cd}_{12}-\text{T3}_6]$ (Figure 2) shows a sharp and very simple pattern, indicating the formation of a discrete assembly with a high degree of structural symmetry. The installed unique methoxy protons of $[\text{T6}_1-\text{Cd}_{12}-\text{T3}_6]$

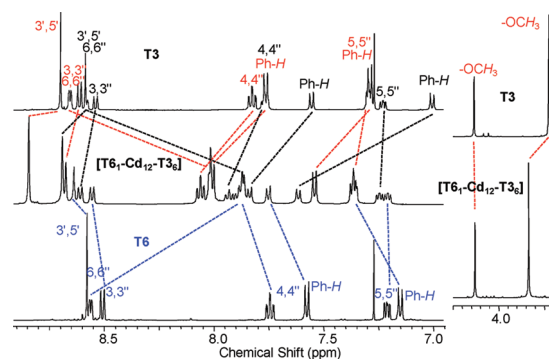


Figure 2. ^1H NMR spectra (500 MHz) of ligands **T3** and **T6** in CDCl_3 and $[\text{T6}_1-\text{Cd}_{12}-\text{T3}_6]$ in CD_3CN .

appear as two singlets at 4.13 and 3.84 ppm in a precise 1:2 ratio. Comparison with the ^1H NMR spectra of free **T6** and **T3** reveals three sets of diagnostic absorptions for the outer (red) and two inner (black and blue) 3',5'-tpy protons (singlet) and 3,3''-tpy protons (doublet) in the expected ratio, which are shifted downfield as a result of the lower electron density upon coordination. The other peaks can be assigned on the basis of the 2D COSY spectra. The 6,6''-tpy proton signals exhibit a dramatic upfield shift relative to the corresponding peaks for the free ligands due to the shielding effect of the metal centers. Interestingly, the 3',5'-tpy protons in the rim show a greater downfield shift than the two sets of tpy protons in the spokes, which might result from the added electron deficiency in the slightly bent outer macrocyclic rim. Moreover, the ^{13}C NMR spectrum of $[\text{T6}_1-\text{Cd}_{12}-\text{T3}_6]$, which contains three peaks for the 3',5'-tpy carbons and two peaks for the methoxy groups, is in full agreement with the wheel's high degree of symmetry. The observed NMR data definitely excluded the presence of both homo-oligomeric byproducts (which were found with $[\text{T6}_1-\text{Zn}_{12}-\text{T3}_6]$) and the free ligands. The related macrocycle $[\text{T2}-\text{Cd}]_4$ was subsequently prepared for comparison (see S13).

In addition to NMR spectroscopy, ESI-MS coupled with traveling-wave ion mobility (TWIM) spectrometry,^{10,16} a variant of ion mobility spectrometry,¹⁷ was applied to validate the proposed structure. $[\text{T6}_1-\text{Cd}_{12}-\text{T3}_6]$ has a molecular weight of 13303.2 Da. The formation of the assembly was confirmed by preliminary ESI-MS, which served as a first-level MS analysis (Figure 3A); a complex with the composition of $[\text{T6}_1-\text{Cd}_{12}-\text{T3}_6]$ was the exclusive isolated product on the basis of the mass-to-charge ratios of the peaks for the major charge states observed ($Z = 7+$ to 14+) and the corresponding isotope patterns (Figure S5). In order to separate any superimposed fragments and determine whether overlapping isomers or conformers of the assembly existed, ESI-TWIM-MS was applied as the second level of MS analysis. As shown in Figure 3B, intact $[\text{T6}_1-\text{Cd}_{12}-\text{T3}_6]$ was the predominant species observed; a few minor fragments were found, but no isomers or conformers were detected. To examine the stability of this spoked wheel, a gradient tandem MS (gMS^2) experiment^{16a} was performed on the assembly ions with charges of 11+ (m/z 1063.4) by subjecting them to collisionally activated dissociation before ion mobility separation at collision energies ranging from 6 to 40 eV (see the SI and Figure S6B). After initially losing the PF_6 units, the 11+ complex ions dissociated further and disappeared completely when the trap voltage reached 40 V, which corresponds to a center-of-mass collision energy (E_{cm}) of 0.14 eV. Application of the gMS^2 method to the 11+

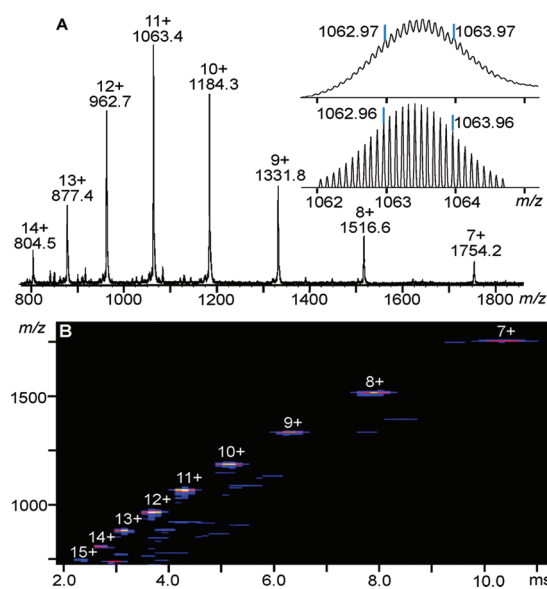


Figure 3. (A) ESI mass spectrum and (B) 2D ESI-TWIM-MS plot (m/z vs drift time) for $[\text{T6}_1\text{-Cd}_{12}\text{-T3}_6]$. The charge states of intact assemblies are marked.

ions of $[\text{T6}_1\text{-Zn}_{12}\text{-T3}_6]$ showed complete dissociation at $E_{\text{cm}} = 0.14$ eV as well (Figure S4C). From the TWIM-MS data, it was possible to derive the collision cross sections (CCSs) of the ions being separated by TWIM (see Figure S7).¹⁸ The CCSs for spoked-wheel ions in various charge states are shown in Table 1. Only slight fluctuations were observed as the charge changed from 6+ to 10+ for $[\text{T6}_1\text{-Cd}_{12}\text{-T3}_6]$ ($1609.7 \pm 46.7 \text{ \AA}^2$) or from 7+ to 10+ for $[\text{T6}_1\text{-Zn}_{12}\text{-T3}_6]$ ($1602.9 \pm 42.6 \text{ \AA}^2$), indicating that such 2D architectures are rigid and shape-persistent. In sharp contrast, our previously reported doughnut-shaped macrocycles, which were generated from a single ligand, showed significant differences in CCS for different charge states,¹⁰ suggesting the existence of various distinct conformers differing in compactness. Thus, $[\text{T6}_1\text{-Cd}_{12}\text{-T3}_6]$ and $[\text{T6}_1\text{-Zn}_{12}\text{-T3}_6]$ must be more rigid and shape-persistent than the related simpler macrocycles. Undoubtedly, the sturdy supporting spoke T6 stabilizes and stiffens the assembly, leading to only minor changes in CCS with charge state. A similar insensitivity of CCS to charge state has been reported by Bowers and co-workers^{17b} for rigid prism structures. It is noteworthy that TWIM-MS not only differentiates ions by mass, charge, and shape but also quantitatively and precisely probes the rigidity of these species through the dependence of the CCS on the charge state.

The structural information deduced from TWIM-MS was corroborated by molecular modeling. Theoretical CCSs for 150 candidate structures of the $[\text{T6}_1\text{-Cd}_{12}\text{-T3}_6]$ spoked wheel (obtained from molecular mechanics/dynamics simulations) were calculated using the projection approximation (PA), trajectory (TJ), and exact hard sphere scattering (EHSS) methods.¹⁹ The resulting plots of CCS versus relative energy (Figure S8) revealed that each of these three methods renders a group of tightly bunched CCSs with a small standard deviation, as listed in Table 1. Most rigorous is the TJ method, which considers both long-range interactions and momentum transfer between the ions and the gas in the ion mobility region, thus providing the most realistic CCS predictions.¹⁹ The CCS obtained for bare $[\text{T6}_1\text{-Cd}_{12}\text{-T3}_6]$ using the TJ model (1750.8 \AA^2) agrees fairly well with the

Table 1. Experimental and Theoretical Collision Cross Sections (CCSs) of Supramolecular Spoked-Wheel Architectures

| Z | CCS (\AA^2) | | |
|-----|------------------------|--|-----------------------------|
| | exptl | exptl avg | calcd avg |
| | | $[\text{T6}_1\text{-Cd}_{12}\text{-T3}_6]$ | |
| 6+ | 1578.6 | | |
| 7+ | 1621.2 | | 1463.6 (8.9), ^a |
| 8+ | 1658.8 | 1609.7 (46.7) | 1464.0 (3.2), ^b |
| 9+ | 1643.7 | | 1750.8 (24.2), ^c |
| 10+ | 1546.0 | | 1801.3 (8.2) ^d |
| | | $[\text{T6}_1\text{-Zn}_{12}\text{-T3}_6]$ | |
| 7+ | 1621.8 | | |
| 8+ | 1638.3 | | |
| 9+ | 1610.0 | 1602.9 (42.6) | |
| 10+ | 1541.3 | | |

^a PA value obtained using DriftScope 2.1. ^b PA value obtained using MOBCAL. ^c TJ value obtained using MOBCAL. ^d EHSS value obtained using MOBCAL.

average experimental CCS for charge states 6+ to 10+ (1609.7 \AA^2). The theory provides a somewhat overestimated value (by $\sim 8.8\%$) because it employs structures without counterions (the precise location of the counterions is unknown). Obviously, the attractive interactions added by the counterions reduce the CCS, albeit only slightly because of the rigidity of the spoked wheel complex.

Transmission electron microscopy (TEM) characterization provided both sizes and shapes of individual molecules upon deposition of a dilute ($\sim 10^{-6}$ M) MeCN solution of $[\text{T6}_1\text{-Cd}_{12}\text{-T3}_6]$ on carbon-coated grids (Cu and Ni, 400 mesh). Individual hexagonal-shaped particles with an average diameter of 6.5 ± 1.0 nm were observed, consistent with the optimized molecular model (Figure 4).

The ligands in dilute CHCl_3 exhibited ligand-centered (LC) $\pi \rightarrow \pi^*$ transitions at 286–291 nm (Figure S12). In comparison with these ligands, the absorption spectra of $[\text{T6}_1\text{-Cd}_{12}\text{-T3}_6]$ and $[\text{T2-Cd}_4]$ ²⁰ (S13) in dilute MeCN showed another distinct absorption band at ~ 323 and ~ 321 nm, respectively, which is assigned to intraligand charge transfer (ILCT). Moreover, the molar extinction coefficient dramatically increased from in going from ligand T3 to $[\text{T6}_1\text{-Cd}_{12}\text{-T3}_6]$, consistent with the corresponding increase in the number of ligands and Cd^{II} metal centers in the molecular wheel. The obvious red shift of the emission maxima in dilute solution for T3 (392 nm) and T2 (398 nm) relative to T6 (368 nm) may be ascribed to electron-donating effects. On the other hand, the emission of $[\text{T6}_1\text{-Cd}_{12}\text{-T3}_6]$ exhibited an obvious red shift and peaked at 462 nm. It is noteworthy that excitation of $[\text{T6}_1\text{-Cd}_{12}\text{-T3}_6]$ at either 284 or 323 nm exclusively gave the same band, suggesting a highly efficient intramolecular energy transfer process.²¹ The macrocycle $[\text{T2-Cd}_4]$ exhibited a significantly weaker emission maximum at ~ 465 nm. Notably, both complexes showed strong fluorescence in thin films, and their emission maxima were red-shifted (36 nm for $[\text{T2-Cd}_4]$, 50 nm for $[\text{T6}_1\text{-Cd}_{12}\text{-T3}_6]$) because of the formation of aggregates in the excited state. The enhanced fluorescence of $[\text{T2-Cd}_4]$ relative to its extremely low emission in solution is attributed to aggregation-induced emission.²²

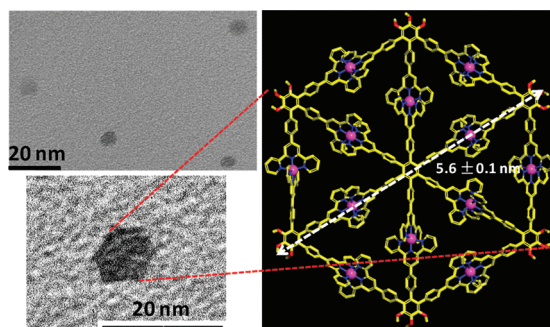


Figure 4. (left) TEM images of $[T6_1-Cd_{12}-T3_6]$ on a carbon-coated Cu grid. (right) Representative energy-minimized structure of $[T6_1-Cd_{12}-T3_6]$.

In conclusion, the first terpyridine-based, shape-persistent, self-assembled 2D D_{6h} supramacromolecular spoked wheel (~ 5.6 nm in diameter) has been prepared in nearly quantitative yield with stoichiometrically and structurally controlled multi-component mixtures of complementary 2,2':6',2''-terpyridine ligands. ESI-MS and TWIM-MS provided unique insight into the size, symmetry, molecular structure, and rigidity of the assembly.

■ ASSOCIATED CONTENT

S Supporting Information. Experimental procedures and characterization data. This material is available free of charge via the Internet at <http://pubs.acs.org>.

■ AUTHOR INFORMATION

Corresponding Author

wesdemiotis@uakron.edu; newkome@uakron.edu

Author Contributions

[§]These authors contributed equally.

■ ACKNOWLEDGMENT

The authors gratefully acknowledge support from the National Science Foundation (DMR-0812337 and DMR-0705015 to G.R.N.; DMR-0821313 and CHE-1012636 to C.W.; DMR-0906898 to S.Z.D.C.). Funding from the Ohio Board of Regents is also acknowledged.

■ REFERENCES

- (1) Wikoff, W. R.; Liljas, L.; Duda, R. L.; Tsuruta, H.; Hendrix, R. W.; Johnson, J. E. *Science* **2000**, *289*, 2129.
- (2) (a) Leininger, S.; Olenyuk, B.; Stang, P. J. *Chem. Rev.* **2000**, *100*, 853. (b) Holliday, B. J.; Mirkin, C. A. *Angew. Chem., Int. Ed.* **2001**, *40*, 2022. (c) Lehn, J.-M. *Science* **2002**, *295*, 2400. (d) Whitesides, G. M.; Grzybowski, B. *Science* **2002**, *295*, 2418. (e) Newkome, G. R.; Wang, P.; Moorefield, C. N.; Cho, T. J.; Mohapatra, P. P.; Li, S.; Hwang, S.-H.; Lukoyanova, O.; Echegoyen, L.; Palagallo, J. A.; Iancu, V.; Hla, S.-W. *Science* **2006**, *312*, 1782. (f) Lee, S. J.; Lin, W. *Acc. Chem. Res.* **2008**, *41*, 521. (g) Zangrado, E.; Casanova, M.; Alessio, E. *Chem. Rev.* **2008**, *108*, 4979.
- (3) (a) Whiteford, J. A.; Fechtenkötter, A.; Stang, P. J. *Nature* **1998**, *398*, 796. (b) Takeda, N.; Umemoto, K.; Yamaguchi, K.; Fujita, M. *Nature* **1999**, *398*, 794. (c) Sun, Q.-F.; Iwasa, J.; Ogawa, D.; Ishido, Y.; Sato, S.; Ozeki, T.; Sei, Y.; Yamaguchi, K.; Fujita, M. *Science* **2010**,

328, 1144. (d) Wang, M.; Zheng, Y.-R.; Ghosh, K.; Stang, P. J. *J. Am. Chem. Soc.* **2010**, *132*, 6282.

(4) (a) Hasenknopf, B.; Lehn, J.-M.; Boumediene, N.; Dupont-Gervais, A.; Dorsselaer, A. V.; Kneisel, B.; Fenske, D. *J. Am. Chem. Soc.* **1997**, *119*, 10956. (b) Hiraoka, S.; Fujita, M. *J. Am. Chem. Soc.* **1999**, *121*, 10239. (c) Schweiger, M.; Seidel, S. R.; Arif, A. M.; Stang, P. J. *Inorg. Chem.* **2002**, *41*, 2556. (d) Kraus, T.; Buddšínský, M.; Cvačka, J.; Sauvage, J.-P. *Angew. Chem., Int. Ed.* **2006**, *45*, 258.

(5) Suzuki, K.; Kawano, M.; Fujita, M. *Angew. Chem., Int. Ed.* **2007**, *46*, 2819.

(6) (a) Christinat, N.; Scopelliti, R.; Severin, K. *Angew. Chem., Int. Ed.* **2008**, *47*, 1848. (b) Northrop, B. H.; Zheng, Y. R.; Chi, K. W.; Stang, P. J. *Acc. Chem. Res.* **2009**, *42*, 1554. (c) Zheng, Y.-R.; Yang, H.-B.; Ghosh, K.; Zhao, L.; Stang, P. J. *Chem.—Eur. J.* **2009**, *15*, 7203. (d) De, S.; Mahata, K.; Schmittel, M. *Chem. Soc. Rev.* **2010**, *39*, 1555.

(7) (a) Armspach, D.; Cattalini, M.; Constable, E. C.; Housecroft, C. E.; Phillips, D. *Chem. Commun.* **1996**, 1823. (b) Newkome, G. R.; He, E.; Godínez, L. A.; Baker, G. R. *J. Am. Chem. Soc.* **2000**, *122*, 9993. (c) Wild, A.; Winter, A.; Schlütter, F.; Schubert, U. S. *Chem. Soc. Rev.* **2011**, *40*, 1459.

(8) (a) Rappas, M.; Schumacher, J.; Beuron, F.; Niwa, H.; Bordes, P.; Wigneshwararaj, S.; Keetch, C. A.; Robinson, C. V.; Buck, M.; Zhang, X. *Science* **2005**, *307*, 1972. (b) Patel, S. S.; Picha, K. M. *Annu. Rev. Biochem.* **2000**, *69*, 651. (c) Pornillos, O.; Ganser-Pornillos, B. K.; Kelly, B. N.; Hua, Y.; Whitty, F. G.; Stout, D.; Sundquist, W. L.; Hill, C. P.; Yeager, M. *Cell* **2009**, *137*, 1282.

(9) (a) Newkome, G. R.; Cho, T. J.; Moorefield, C. N.; Mohapatra, P. P.; Godínez, L. A. *Chem.—Eur. J.* **2004**, *10*, 1493. (b) Hwang, S.-H.; Wang, P.; Moorefield, C. N.; Jung, J.-C.; Kim, J.-Y.; Lee, S.-W.; Newkome, G. R. *Macromol. Rapid Commun.* **2006**, *27*, 1809.

(10) (a) Wang, J.-L.; Li, X.; Lu, X.; Chan, Y.-T.; Moorefield, C. N.; Wesdemiotis, C.; Newkome, G. R. *Chem.—Eur. J.* **2011**, *17*, 4830. (b) Chan, Y.-T.; Li, X.; Moorefield, C. N.; Wesdemiotis, C.; Newkome, G. R. *Chem.—Eur. J.* **2011** in press.

(11) (a) Rucareanu, S.; Schuway, A.; Gossauer, A. *J. Am. Chem. Soc.* **2006**, *128*, 3396. (b) Jung, S.-H.; Pisula, W.; Rouhanipour, A.; Räder, H. J.; Jacob, J.; Müllen, K. *Angew. Chem., Int. Ed.* **2006**, *45*, 4685. (c) Mössinger, D.; Hornung, J.; Lei, S.; De Feyter, S.; Höger, S. *Angew. Chem., Int. Ed.* **2007**, *46*, 6802. (d) O'Sullivan, M. C.; Sprafke, J. K.; Kondratuk, D. V.; Rinfray, C.; Claridge, T. D. W.; Saywell, A.; Blunt, M. O.; O'Shea, J. N.; Beton, P. H.; Malfois, M.; Anderson, H. J. *Nature* **2011**, *469*, 72.

(12) Schmittel, M.; Mal, P. *Chem. Commun.* **2008**, 960.

(13) Jarosz, P.; Lotito, K.; Schneider, J.; Kumaresan, D.; Schmehl, R.; Eisenberg, R. *Inorg. Chem.* **2009**, *48*, 2420.

(14) Mora, M.; Jiménez-Sanchidrián, C.; Ruiz, J. R.; Bauer, T.; Schlüter, A. D.; Sakamoto, J. *Synlett* **2010**, 877.

(15) Chan, Y.-T.; Li, X.; Soler, M.; Wang, J.-L.; Wesdemiotis, C.; Newkome, G. R. *J. Am. Chem. Soc.* **2009**, *131*, 16395.

(16) (a) Li, X.; Chan, Y.-T.; Newkome, G. R.; Wesdemiotis, C. *Anal. Chem.* **2011**, *83*, 1284. (b) Perera, S.; Li, X.; Soler, M.; Schultz, A.; Wesdemiotis, C.; Moorefield, C. N.; Newkome, G. R. *Angew. Chem., Int. Ed.* **2010**, *49*, 6539.

(17) (a) Hoaglund-Hyzer, C. S.; Counterman, A. E.; Clemmer, D. E. *Chem. Rev.* **1999**, *99*, 3037. (b) Bocker, E. R.; Anderson, S. E.; Northrop, B. H.; Stang, P. J.; Bowers, M. T. *J. Am. Chem. Soc.* **2010**, *132*, 13486.

(18) Thalassinou, K.; Grabenauer, M.; Slade, S. E.; Hilton, G. R.; Bowers, M. T.; Scrivens, J. H. *Anal. Chem.* **2009**, *81*, 248.

(19) (a) Shvartsburg, A. A.; Jarrold, M. F. *Chem. Phys. Lett.* **1996**, *261*, 86. (b) Jarrold, M. F. *Annu. Rev. Phys. Chem.* **2000**, *51*, 179. (c) Shvartsburg, A. A.; Liu, B.; Siu, K. W. M.; Ho, K.-M. *J. Phys. Chem. A* **2000**, *104*, 6152.

(20) Bugarin, A.; Connell, B. T. *Organometallics* **2008**, *27*, 4357.

(21) (a) Pei, J.; Wang, J.-L.; Cao, X.-Y.; Zhou, X.-H.; Zhang, W.-B. *J. Am. Chem. Soc.* **2003**, *125*, 9944. (b) Wang, J.-L.; Yan, J.; Tang, Z.-M.; Xiao, Q.; Ma, Y.; Pei, J. *J. Am. Chem. Soc.* **2008**, *130*, 9952.

(22) Hong, Y.; Lam, J. W. Y.; Tang, B. Z. *Chem. Commun.* **2009**, 4332.